

Content from this work may be used under the terms of the CC BY 3.0 licence (© 2019). Any distribution of this work must maintain attribution to the author(s), title of the work, publisher, and DOI.

THE FRIB SC-LINAC: INSTALLATION AND PHASED COMMISSIONING*

J. Wei[#], H. Ao, S. Beher, B. Bird, N. Bultman, F. Casagrande, D. Chabot, W. Chang, S. Cogan, C. Compton, J. Curtin, E. Daykin, K. Davidson, K. Elliott, A. Facco¹, A. Fila, V. Ganni, A. Ganshyn, P. Gibson, T. Glasmacher, I. Grender, W. Hartung, L. Hodges, K. Holland, H.-C. Hseuh, A. Hussain, M. Ikegami, S. Jones, T. Kanemura, S.-H. Kim, M. Konrad, P. Knudsen, R.E. Laxdal², J. LeTourneau, Z. Li, S. Lidia, G. Machicoane, P. Manwiller, F. Marti, T. Maruta, E. Metzgar, S. Miller, D. Morris, C. Nguyen, K. Openlander, P. Ostroumov, A. Plastun, J. Popielarski, L. Popielarski, J. Priller, M. Reaume, H. Ren, T. Russo, K. Saito, M. Shuptar, J. Stetson, D. Victory, R. Walker, X. Wang, J. Wenstrom, M. Wright, M. Xu, T. Xu, Y. Yamazaki, Q. Zhao, S. Zhao, Facility for Rare Isotope Beams, Michigan State University, East Lansing, MI, USA

K. Dixon, M. Wiseman, Thomas Jefferson National Laboratory, Newport News, VA, USA

M. Kelly, Argonne National Laboratory, Argonne, IL, USA

K. Hosoyama, KEK, Tsukuba, Japan

¹also at INFN - Laboratori Nazionali di Legnaro, Legnaro (Padova), Italy

²also at TRIUMF, Vancouver, Canada

³also at Argonne National Laboratory, Argonne, IL, USA

Abstract

The Facility for Rare Isotope Beams (FRIB) superconducting (SC) radio-frequency (RF) driver linac is designed to accelerate all stable ions, including uranium, to energies above 200 MeV/u. The linac includes 46 cryomodules (CMs) containing 104 quarter-wave resonators (QWRs) and 220 half-wave resonators (HWRs). With the newly-commissioned refrigeration system supplying liquid helium to the QWR and SC solenoids, heavy ion beams including Ne, Ar, Kr, and Xe were accelerated to > 20 MeV/u in the first linac segment (LS1), using 15 CMs containing 104 QWRs ($\beta = 0.041$ and 0.085) and 39 solenoids. Even at this intermediate stage, the FRIB accelerator has already become the world's highest-energy continuous-wave (CW) hadron linac [1]. Installation of HWR CMs ($\beta = 0.29$ and 0.53) is proceeding in parallel. Development of $\beta = 0.65$ elliptical resonators is on-going to support an energy upgrade to 400 MeV/u. This paper summarizes the FRIB SC-linac installation and phased commissioning status that is on schedule and on budget.

INTRODUCTION

The Facility for Rare Isotope Beams (FRIB) driver linac uses SRF technology to accelerate CW or pulsed beams of stable ions, from hydrogen to uranium, from 0.5 MeV/u to 200 MeV/u, with upgrade potential to 400 MeV/u [2]. Four types of accelerating cryomodules (CMs) are used, all operating at 2 K: $\beta = 0.041$ and 0.085 QWRs at 80.5 MHz, and $\beta = 0.29$ and 0.53 HWRs at 322 MHz (Fig. 1). The CMs also contain SC solenoid packages operating at 4.5 K for transverse focusing and steering.

Strategically-designed segmentation in the cryo-distribution system facilitates phased commissioning with

parallel installation and maximizes machine availability and maintainability. The helium refrigeration system feeds cryogens through four separated distribution lines, one for each of the three linac segments (LS1 to LS3) and the fourth for the experiment systems (ES) area. U-tube connections allow for flexible and robust configuration changes. Each CM is connected to via U-tubes, allowing independent cool-down and warm-up of each CM. The segmented design provides the flexibility needed for phased commissioning: LS1 (Fig. 1, red) remains cold since April 2019 after beam commissioning; LS2 (Fig. 1, blue) is being cooled down in preparation for beam commissioning; LS3 (Fig. 1, green) is under fabrication and installation; and the ES (Fig. 1, brown) area cryogenic and magnet systems are still being designed (Table 1).

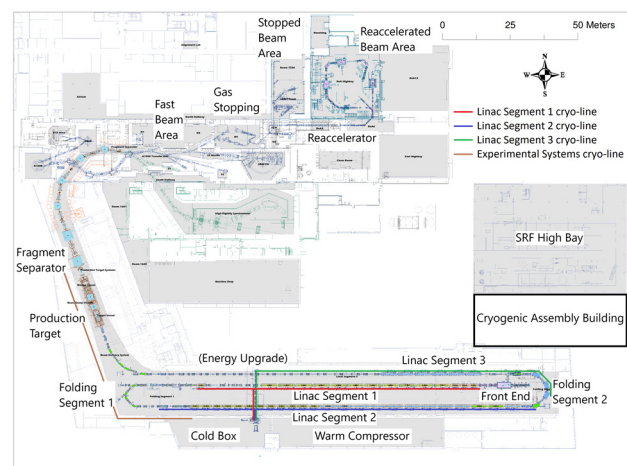


Figure 1: Schematic layout of the FRIB accelerator complex. The primary beam is generated from the front end and accelerated through linac segment 1 (LS1), folding segment 1 (FS1), LS2, FS2, and LS3, then strikes the production target for rare isotope production of fast, stopped, and reaccelerated beams.

*Work supported by the U.S. Department of Energy Office of Science under Cooperative Agreement DE-SC0000661.

[#]wei@frib.msu.edu

An innovative “bottom-up” cryomodule design facilitates the mass production required for the SC-linac CMs. The cold mass is mounted on supporting posts on linear roller bearings to streamline CM assembly and alignment [3, 4]. The cryogenic headers are suspended from the top for microphonics suppression. Local magnetic shielding allows the solenoids to operate at ~ 8 T without compromising the resonator performance.

Rigorous acceptance testing is employed to ensure quality accelerator components for rapid beam commissioning. Extensive development work and pre-production prototyping were done for both sub-components (cavities, couplers, tuners, solenoids) and CMs. Subsequently, all production sub-components are tested before assembly onto a cold mass. Each assembled cryomodule is bunker tested before tunnel installation [5].

Table 1: Stages of Accelerator Readiness (ARR) for the Phased Beam Commissioning of the FRIB Accelerator

| ARR Phase | Area with beam | Energy MeV/u | Date |
|-----------|------------------------------|--------------|----------|
| 1 | Front end | 0.5 | Jul 2017 |
| 2 | + $\beta = 0.041$ | 2 | May 2018 |
| 3 | + $\beta = 0.085$ (LS1) | 20 | Feb 2019 |
| 4 | + $\beta = 0.29, 0.53$ (LS2) | 200 | Mar 2020 |
| 5 | + $\beta = 0.53$ (LS3) | >200 | Dec 2020 |
| 6 | + target, beam dump | >200 | Sep 2021 |
| Final | integration with NSCL | >200 | Jun 2022 |

DESIGN AND CONSTRUCTION

Helium Refrigeration System

The initial plan of a “turn-key” approach for the cryogenic helium system from industry exposed the project to serious risks in budget and scope. The approach failed since a large-scale, non-standard system is not a manufacturer’s standard product; many required subsystems are not the primary contractor’s expertise. This lead FRIB to utilize the design and operations experience of JLab and SNS and to acquire expertise accordingly to form an in-house team.

The FRIB cryogenic system, integrating the cryo-plant (Fig. 2), cryo-distribution, and cryomodules is based on a modular design to support phased installation and commissioning. At the cryogenic plant level, the distribution system is divided into four main branches, as shown in Figure 1. All interfaces between the cryo-plant and the four main distribution branch lines are connected using a pair of cryogenic couplings that are connected by a removable inverted U-tubes with ambient temperature valves for isolation when U-tubes are removed. Each cryogenic load is also connected to the main distribution with U-tubes for each circuit (i.e., 4.5 K helium supply, 4.5 K helium return, shield supply, shield return, sub-atmospheric return, etc.). The cryo-plant uses the Ganni floating pressure process, allowing both the compressor discharge and 4.5 K cold box supply pressure to automatically vary from 6 to 21 bar without introducing

additional loads or exergetic losses [6]. This allows for efficient operation with reduced loads during commissioning or as dictated by operational needs, since the main compressor input power is mainly proportional to the supply pressure to the cold box. The main compressor skid design was developed for the NASA James Webb project. The 2 K (31 mbar) load is supported using five stages of centrifugal cryogenic compressors, housed within the sub-atmospheric cold box that recompress the helium to 1.15 bar (~ 30 K), with reinjection of the discharge into the 4.5 K cold box. The 4.5 K cold box is comprised of two separate vacuum-insulated vessels, a vertical one that spans from 300 K to 60 K and a horizontal one housing seven turbines with four expansion stages and a sub cooler. This cold box has an equivalent 4.5 K refrigeration capacity of 18 kW.

Most of the subsystems were designed by the FRIB cryogenic design team consisting of members from JLab and MSU, and procured from the industry as build-to-print. The team is also responsible for the planning, integration, installation, controls, commissioning, and operations of the entire system. Careful planning and execution avoided the need to store or “double-handle” any equipment. The 4.5 K refrigeration system, operating with the main compressors, met all the design goals and has been continuously operating since April 2018, efficiently supporting the phased commissioning of the SC-linac. Similarly, the 2 K system was tested in December 2018 and met all the design goals for linac operations.

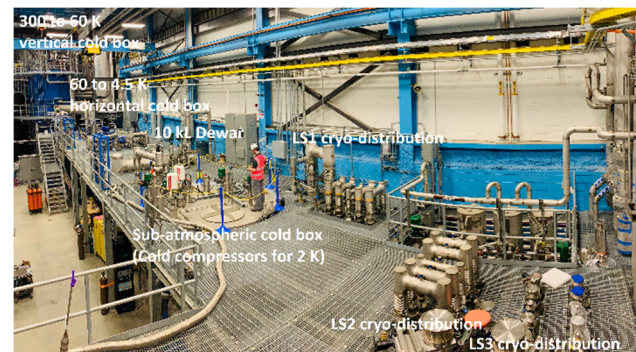


Figure 2: FRIB cryoplant operating at both 4.5 K and 2 K temperatures.

Quarter-wave Resonator Cryomodules

SRF cryomodules are designed to accelerate CW ion beams starting from 0.5 MeV/u energy. LS1 uses 15 QWR cryomodules containing 104 QWRs of $\beta = 0.041$ and 0.085 and 39 solenoids to accelerate the beam through the charge stripper to the beam dump at FS1 (Figs. 1 and 3).

FRIB superconducting resonators are double-wall, coaxial cavities made of bulk niobium and surrounded by a titanium He vessel [7]. To meet the FRIB construction and long-term operation needs, the design philosophy aims at a good balance between high reliability and performance, easy production and assembly, and low cost. Design complications have been carefully avoided. The Ti vessel is a fundamental component of the structure and contributes to its mechanical stability. Nb and Ti are

Content from this work may be used under the terms of the CC BY 3.0 licence (© 2019). Any distribution of this work must maintain attribution to the author(s), title of the work, publisher, and DOI.

directly welded together. The cavity preparation includes a bulk etch (BCP), 650 °C thermal treatment followed by a light etch, and high-pressure water rinsing in a clean room. Following our test results, we decided to apply 120 °C baking only to the ReA QWRs (operating at 4.5 K) but not for the FRIB cavities operating at 2 K, as no real improvement was observed after baking. Cavity final frequency adjustment includes plastic deformation, differential etching and virtual welding when needed.

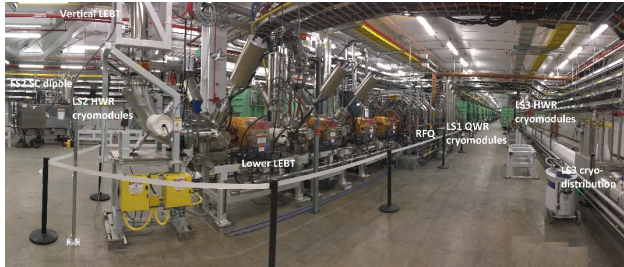


Figure 3: Photograph of the FRIB tunnel during ARR3 beam commissioning. The beams down from the vertical LEBT are accelerated through the RFQ and the LS1 QWR cryomodules to the beam dump at the end of LS1.

Cavity development work intensified in 2011, prompted by an unforeseen lack of performance of the first lot of $\beta = 0.085$ QWRs. A systematic testing campaign finally identified a subtle flaw in the first generation QWR design: where a combination of design choices was leading to overheating, bad rf contact and problematic differential contraction [8]. All cavity designs, including HWRs, were thoroughly revised. For the QWRs, the rf couplers were moved from the tuning plate to the side; the tuning plate was moved further away from the inner conductor, and the bottom flange design and materials were changed. This solved the design problems, and eight underperforming QWRs were fully recovered and installed in the ReA linac. In addition, the electromagnetic, cryogenic and mechanical design of all cavities were re-optimized, improving their performance and allowing a slight reduction of in the cavity count and a larger safety margin for performance. The initial rather complex HWR tuner was replaced by an Argonne-type pneumatic one [9], with a newly designed interface to the cavity which allows for easy installation in the tight space available between cavities after cold mass assembly. The fundamental power couplers (FPCs) for the QWRs and HWRs were modified and upgraded. An Argonne-style 4 kW double window adjustable FPC design was adopted for QWRs; in the SNS-type, single-window FPC used for HWRs, the impedance profile was modified to reduce multipacting conditioning time. The resonator construction and tuning procedures, surface processing, and thermal treatments were updated as well. A rigorous validation procedure, including integrated resonator testing in operation-like conditions, was set up and enforced in the production chain. This rather intensive campaign required a considerable effort, but succeeded in meeting all FRIB requirements in due time.

The cryomodule design converged to a single approach for all cavity types after testing of the first generation, “top-down” QWR and HWR cryomodule prototypes. In the first generation, the assembly time was found to exceed by far the time allocated in the FRIB schedule. The new “bottom-up” design [10] allows for an easier, faster and more reproducible assembly procedure, and gives better access to cavities and ancillaries during critical assembly steps (Fig. 4). The rather long cold mass alignment rails, split in two or three independent sections to limit thermal displacements, sit on short G10 posts which stand directly on the cryomodule baseplate, which supports all rf, cryogenic and beam vacuum interfaces. A clever system of linear bearings placed in between posts and rails provides automatic alignment of the cold mass to the beam axis during cool-down with excellent precision and reproducibility. The cryomodule top cover has only the functions of vacuum vessel and of stiff support for the helium reservoir. To validate the new design and the required long O-ring seal with 3-way connections, a special cryomodule mockup (“engineering test cryomodule,” ETCM) was built and tested to verify the kinematic support and post-cool-down alignment accuracy.

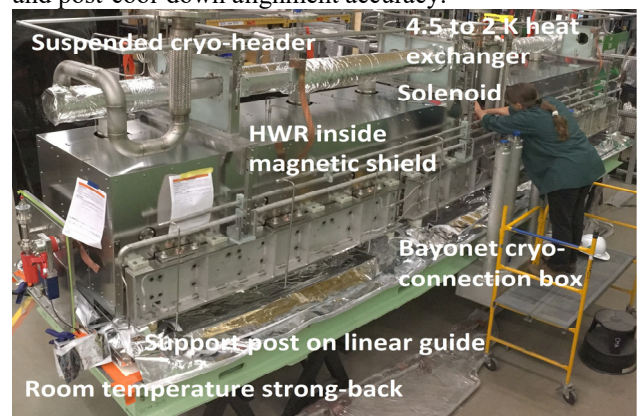


Figure 4: Partially assembled $\beta = 0.53$ cryomodule. The base-plate, alignment rails, thermal shield, cryogenic headers, and cryogenic connections are visible.

INSTALLATION AND PREPARATION

Installation and system integration must be completed before device readiness reviews (DRR) are conducted; after DRR, integrated tests are done, followed by accelerator readiness reviews (ARR) prior to beam commissioning. Each DRR consists of device hazard and device operation reviews. These activities are concerted for each phase of commissioning listed in Table 1.

Personnel Protection System

Personnel protection systems include oxygen deficiency hazard (ODH) control, the access control system (ACS), and the radiation control system (RCS) [11]. The ODH control system is sequentially deployed in the cryoplant building before the cryoplant commissioning, in the linac tunnel before cooling down, and in the service building above the tunnel due to unsealed conduits. The ACS is deployed before high power RF conditioning of SRF

cavities. The RCS is deployed in steps according to the beam energy during beam commissioning (Table 1).

Cryo-Distribution Installation

The cryomodule has loads at 3 different temperatures, requiring 5 process circuits in the distribution system: a 4.5 K supply (for cryomodules and SC magnets), a 4.5 K return (1.2 bar, for SC magnets), a 4 K return (0.03 bar, 2 K flow from cryomodules after energy exchange with the 4 K supply flow in the 2 K – 4 K heat exchanger), a 40 K shield supply, and 55 K shield return. The goal is to maintain flexibility to connect or disconnect any cryogenic load at any time to support installation, phased commissioning, and maintenance. Each linac segment has cryogenic coupling U-tube interface at the cryogenic plant, a shaft transfer line from the cryoplant to the tunnel, a horizontal line to a tee for each segment and a connection for each cryomodule on either side of the tee. Figure 5 shows the LS1 cryo-distribution scheme. The design for the cryogenic line with cryogenic couplings and cryogenic control valves was standardized. Forty-six of these sections were procured from industry and are being installed in the three linac segments to interface with the cryomodules [12].

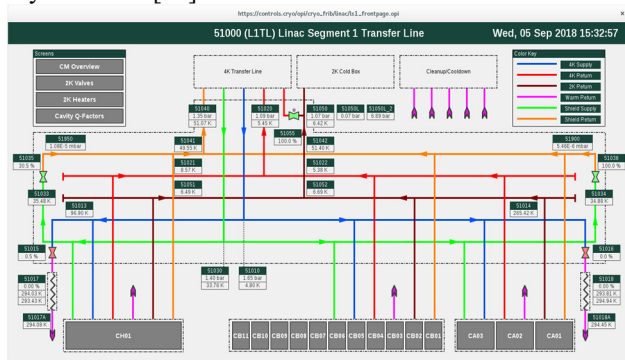


Figure 5: Cryo-distribution schematic for LS1.

Cryomodule Tests and Transportation

Jacketed FRIB resonators are etched, rinsed, and Dewar tested at MSU [13 - 15]. After Dewar certification testing, the resonators and RF couplers are installed onto a cold mass [16] and assembled into a cryomodule. Each cryomodule undergoes cryogenic and RF testing at MSU before installation into the FRIB tunnel. Cryomodule testing [17] verifies operation of the cavities, couplers [18], tuners [10], solenoid packages [19, 20], magnetic shield, and thermal shield at 4.3 K and 2 K.

Detailed procedures have been developed to move the cryomodules safely [4, 21], though the risk is relatively low since the FRIB CMs are assembled and bunker tested in house, ~ 100 m from the final installed locations. The CMs are transported with the beam line/cavity space under vacuum and with the insulating space vented to nitrogen gas. The beam line vacuum is actively pumped with a battery-powered ion-getter pump when the CM is being moved. Accelerometers are attached to the CMs for their journey from the test bunker to the linac tunnel. CMs are moved between buildings on a truck; they are lowered into

the tunnel with a crane. They are moved into their final position in the tunnel on wheels, using a self-propelled crawler drive. Once the CM is in its final position, the wheels are replaced with stationary supports. The supports allow for fine adjustment of the position for cryomodule alignment [5].

Survey and Alignment

The “bottom-up” design and assembly approach for achieving internal alignment of cavities and solenoids within each cryomodule provides most of the internal cold mass alignment with minimal manual intervention. This technique saves assembly time and proves suitable for mass production. Cavity and solenoid fiducials are measured at room temperature during assembly and related to baseplate fiducials before cold mass visibility is lost due to installation of the vacuum cover. Thermal offset corrections are applied to the room temperature CM assembly measurements to account for the effect of cool-down. A least-squares best fit line through the magnetic centers of the solenoids is used to characterize the primary axis to align each CM. Figure 6 shows the expected cavity and solenoid as-aligned positions from the ideal beam trajectory considering: (i) solenoid mapping magnetic offset data; (ii) cavity and solenoid fiducialization data; (iii) assembly measurements relating cavity and solenoid fiducials to CM baseplate fiducials; (iv) cool down offset corrections; (v) measured baseplate distortion between assembly, vacuum cover installation, transport; (vi) as-aligned baseplate fiducial measurements. The expected cavity and solenoid position deviations are 0.29 ± 0.16 mm and 0.42 ± 0.20 mm, respectively. Solenoid alignment is prioritized to minimize mis-steering.

LS1 alignment was validated and quantified during beam commissioning, which only required 25% of available corrective dipole current to steer the beam on-axis within ± 1 mm. The alignment procedures consist of fiducializing each beam component during assembly, establishing a robustly-measured network of survey monuments surrounding the beam line, and positioning beam components on the theoretical beam line with sub-millimeter placement tolerance by referencing component fiducials relative to the monument network.

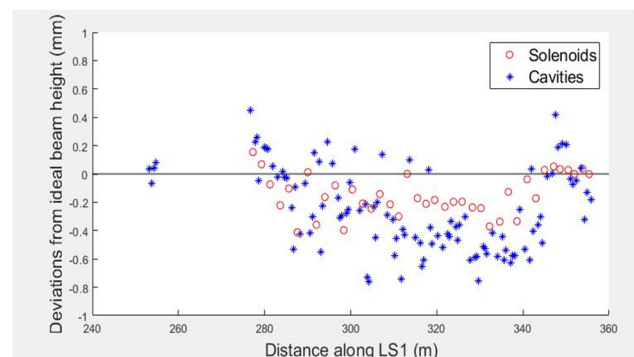


Figure 6: Expected LS1 cavity and solenoid as-aligned vertical displacements from the ideal beam trajectory.

Content from this work may be used under the terms of the CC BY 3.0 licence (© 2019). Any distribution of this work must maintain attribution to the author(s), title of the work, publisher, and DOI.

Cryo-Distribution and Cryomodule Cool-Down

The integrated LS1 cryo-distribution was first cooled to operating temperatures. Subsequently, the cryo-distribution was connected to the first 3 cryomodules by U-tubes and the CMs were cooled to operating temperatures. The beam was accelerated through these 3 cryomodules in ARR2, establishing the base line for the beam operations. Later, the remaining 12 CMs of LS1 were connected to the cryo-distribution and cooled to operating temperatures with the first 3 CMs still cold. Presently, LS2 and LS3 are connected to their respective tee sections, the shaft sections, and the cryogenic coupling sections in the cold box room. The LS2 transfer line has been cooled and supported the commissioning of the first SC dipole magnet at the East end of the LS2 transfer line, which is ready for CM connections.

Microphonics Mitigation

Because of the narrow bandwidth of SRF cavities, microphonic excitation is a potential show-stopper. Hence microphonic mitigations were implemented starting at the system design stage for both cryogenics and cryomodules. In addition to a careful cavity and CM design, several specific features were incorporated: (i) all QWRs were equipped with mechanical dampers; (ii) the long helium headers in the CMs were firmly connected to the CM top covers to efficiently suppress their low-frequency mechanical modes; (iii) the 2 K operation temperature was extended—for the first time in a SC linac, and without significant loss of overall cryogenic efficiency—to the QWR section to reduce helium bath pressure fluctuations and related microphonics by more than one order of magnitude. Smooth operation of tuners and cryogenic valves was adopted as well.

Suppression of cryogenic compressor vibration is monitored by tunnel measurements of the vibration spectrum (Fig. 7). The results indicate that we are able to meet the requirement of < 40 nm rms amplitude over the relevant frequency range. In the initial cool-down some SRF cavity locking issues were observed. These were promptly resolved by iterative improvements in the valve control logic and by provisions for 1.6 bar liquid helium from a 10k liter Dewar, instead of from the 3 bar super-critical supply.

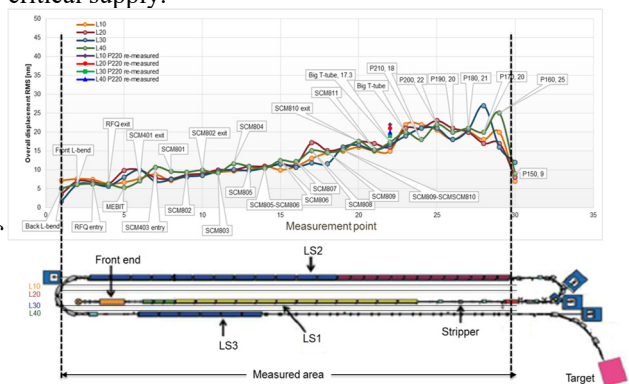


Figure 7: Measured tunnel vibration after the turn on of the cryoplant compressors.

Device Energization and RF Conditioning

The smooth SRF commissioning was possible only because extensive tests were first conducted on individual components and then on integrated systems to resolve potential issues. For example, slow frequency tuner operation and microphonics were checked in LLRF integration tests [22]; the frequency-tracking circulator integrated in the RF amplifier was tested in amplifier tests [23]. High-power RF operation of the cavities started with RF interlock tests and field calibration checks, followed by multipacting conditioning and field emission X-rays checks. Multipacting conditioning took about 1 hour per cryomodule (with up to 8 cavities), as multiple cavities can be simultaneously conditioned while keeping the dynamic load into the helium bath at a moderate level. No cavities had high field emission X-rays, so no field emission conditioning was performed. In addition, there were no measurable changes in the field emission X-rays before and after opening the beam line gate valves [22]. After all of the tests, checks, and measurements, stable amplitude and phase lock at the design field was demonstrated along with operation of the slow frequency tuner.

During CM commissioning, all SC solenoids and correctors were energized to ~ 80% of the full design current while PID control parameters were optimized on the helium gas flow for cooling the current leads. During beam commissioning, solenoids were set at 20 to 70% of the full field (8 T), and correctors were set at ~ 10% of full field for beam tuning. The SC magnet packages had no quenches during LS1 beam commissioning.

Low-level RF Controls

The FRIB LLRF controller is designed to accommodate various cavity and tuner types [23]. Using direct-sampling / under-sampling allows the analog-to-digital converter (ADC) to sample RF signals of five different frequencies ranging from 40.25 MHz to 322 MHz with the same sampling frequency. RF output synthesis is done using three RF board variations, each supporting two frequencies. Two types of tuner boards of the same form factor are designed to drive 2-phase or 5-phase stepper motors for the QWR and multi-gap buncher (MGB), respectively, and to drive analog tuners (pneumatic valves for HWR, tuner error signal for RFQ). Besides flexibility, other LLRF controller features include a digital self-excited loop (SEL), allowing cavities to be driven with tuners unlocked; advanced control algorithms for high performance [24]; comprehensive external and internal interlocks to protect the cavities, amplifiers, and other equipment; and an auto-start procedure to automate cavity turn-on for efficient operation (Fig. 8).

During ARR3 commissioning, over 100 SRF cavities were turned on and ready for beam in less than 30 minutes. Without beam, the amplitude and phase peak error were better than $\pm 0.1\%$ and $\pm 0.2^\circ$, respectively, well below the requirement of $\pm 1\%$ and $\pm 1^\circ$. At ~ 30% final peak current, the amplitude regulation is still better than $\pm 0.2\%$. Beam loading effects on phase regulation are negligible.

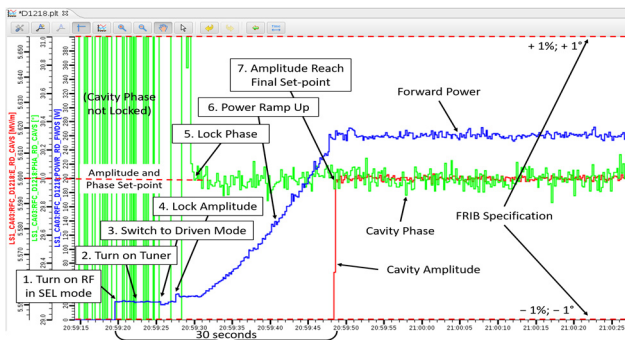


Figure 8: Example of automated turn-on of QWR during ARR3 commissioning.

Instrumentation and Machine Protection

Beam instrumentation and diagnostics in LS1 consist of room temperature and cryogenic button-style BPMs [25], AC current transformers (ACCTs), halo monitor rings [26], fast thermometry sensors on the cryomodule beam pipe, and scintillator-based neutron monitors for beam loss detection. Most signals are read by MicroTCA [27] for analysis and decision-making. A mixture of commercial and in-house custom hardware and firmware are used to integrate global timing, RF clock, machine protection, and data acquisition and reporting [28, 29].

The beam pulse structure is generated by an electrostatic chopper in the Front End [30]. The chopper system provides the operator with a high-precision (to 12.4 ns) knob to tune the pulse duration and duty cycle, assisted by an FPGA-based chopper monitor. Typically, beam commissioning is done with a 50 μ s pulse at 100 Hz, though higher duty cycles have been used for higher average power tests.

The fast machine protection system safeguards the cryomodules and ensures that the operational safety envelope parameters are strictly observed [31, 32]. During low-power commissioning (beam power < 2 W), the ACCT network monitors the peak beam intensity as well as differential beam losses throughout LS1. The beam is inhibited within 35 μ s upon over-power or power-loss-over-threshold conditions (Fig. 9), or from fast events detected by the LLRF controllers [32]. During high-power operation, additional modalities of beam loss detection (halo rings, neutron monitors, etc.) provide additional layers of safety.

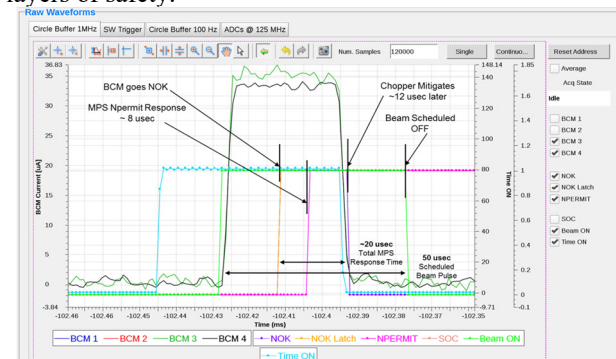


Figure 9: Demonstration of fast machine protection with the differential current monitor signal.

Facilities - Progress

status report of funded machines

Control Software Deployment

Control software packages are automatically built on a continuous integration cluster and deployed in a manner which is tightly integrated with FRIB's information technology infrastructure management system [33]. This allows software to be deployed frequently and in a reproducible way, making it possible to address software development needs identified during beam commissioning in a timely manner.

PHASED BEAM COMMISSIONING

Phased beam commissioning started in 2017, three years after the start of FRIB technical construction (Critical Decision 3). Each of the 7 commissioning phases, listed in Table 1, carries specific goals, and is preceded by an accelerator readiness review (ARR). ARR1 established the commissioning team culture and integrated warm accelerator systems with newly-built civil infrastructure [34]. ARR2 integrated the cryogenic refrigeration system with the CMs and other accelerator systems. ARR3 transformed the accelerator tunnel into a radiation restricted area, with acceleration of multiple species and ion charge states to > 20 MeV/u. ARR4 aims at fully commissioning the cryogenic system with both 4 K and 2 K operations and accelerating ions to 200 MeV/u with both QWR and HWR CMs. ARR5 marks the completion of linac commissioning and readiness to transfer beams to the experimental area.

All 104 QWRs in the fifteen LS1 cryomodules met the design accelerating gradients (5.1 MV/m for $\beta = 0.041$ QWRs and 5.6 MV/m for $\beta = 0.085$ QWR) with no field emission or multipacting issues [22]. The twelve $\beta = 0.085$ CMs were commissioned at a rate of about 1 cryomodule per day with 8 hour shifts. High-power RF operation of the LS1 SRF cavities was done at 4.5 K, a more challenging condition for microphonics than the baseline design (2 K).



Figure 10: ARR3 beam commissioning in 2019 in the FRIB main control room.

Linac Segment 1 Beam Commissioning

LS1 beam commissioning (Fig. 10) met all goals ahead of the baseline schedule. In ARR1 and ARR2, detailed studies of beam dynamics in the Front End and the first three cryomodules were done, as reported in Ref. [35].

For ARR3, three one-week beam shifts were scheduled from February to April 2019, alternating with ongoing equipment installation in the tunnel. Starting with low beam power (< 2 W), we applied a phase scan procedure to all 104 SC cavities to accelerate an argon ion beam ($^{40}\text{Ar}^{9+}$) to 20.3 MeV/u. The transverse beam dynamics were

Content from this work may be used under the terms of the CC BY 3.0 licence (© 2019). Any distribution of this work must maintain attribution to the author(s), title of the work, publisher, and DOI.

verified by beam profile measurements and evaluation of the Courant-Snyder parameters and rms emittances. Beams of $^{20}\text{Ne}^{6+}$, $^{86}\text{Kr}^{17+}$ and $^{129}\text{Xe}^{26+}$ were accelerated to 20.3 MeV/u by simple scaling of all electromagnetic fields according to the charge-to-mass ratio relative to the settings for $^{40}\text{Ar}^{9+}$. The beam transmission through LS1 was 100% for all beams with measurement uncertainty < 1%. The beam-charge-state distributions after the stripper were measured via a 45° bending magnet and charge-state selection slits.

The maximum allowable beam power is limited to 500 W by the air-cooled beam dump at folding segment 1 (FS1). We delivered high-power equivalent beam to the beam dump in two modes: pulsed and CW. Initially, a pulsed Ar beam with peak intensity of 3.8 pμA and 10% duty cycle was accelerated and delivered to the beam dump. Then the peak intensity was increased to 14.8 pμA which (30% of the FRIB design goal) at 3% duty factor. In CW, a 0.36 pμA beam of Ar was accelerated, which set a new world record for the highest-energy CW superconducting hadron linac.

A number of accelerator physics tools were successfully tested, including central trajectory correction with the “optics response matrix” (ORM) method, phase scan and field calibration procedures, and on-line beam matching using profile monitor data. Figure 11 shows signals in the beam position monitors (BPMs) along LS1 with manual tuning (top) and with ORM-based beam steering correction (bottom). The ORM method allows for a significant reduction in the transverse displacement. We used 133 μA beam pulses of duration 6 ms to test the low-level RF (LLRF) system’s capacity to compensate for beam loading. The LLRF control system kept the cavity voltage constant with an accuracy of < 0.1%.

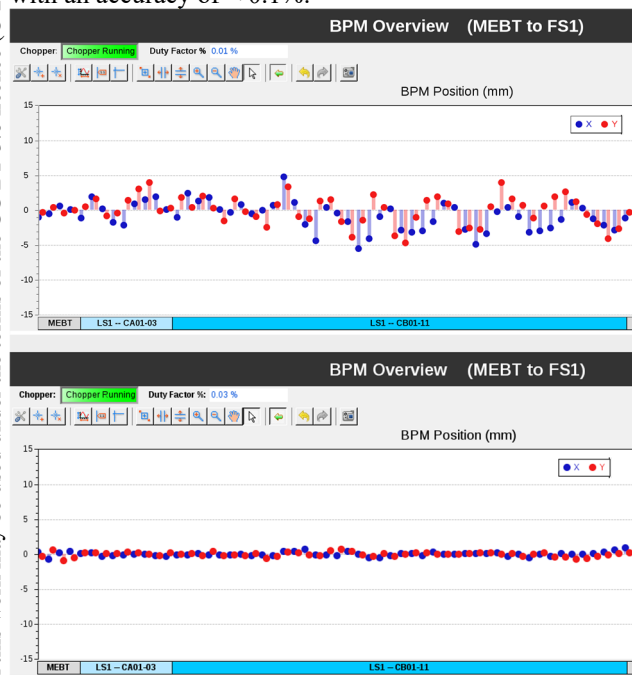


Figure 11: Horizontal and vertical beam centroid positions for an Ar beam along LS1 measured by the BPMs after

manual correction (top) and after ORM-based steering correction (bottom).

Forthcoming Beam Commissioning

ARR4, scheduled for March 2020, aims at accelerating heavy ion beams like Ar to about 200 MeV/u using the 15 QWR CMs in LS1 and 24 HWR CMs in LS2 (12 $\beta = 0.29$ CMs and 12 $\beta = 0.53$ CMs). Subsequent ARRs aim at accelerating the primary beam with the remaining six HWR CMs, transporting the beam through the space reserved in LS3 for the FRIB energy upgrade, striking the production target, producing the rare-isotope secondary beam, and transporting through the new fragment separator and reconfigured experimental areas (Table 1).

OPERATIONS COORDINATION

Operations coordination is key to mitigate safety hazards during interlaced beam commissioning and installation. During commissioning shifts, the ACS prevents access into the shielded enclosure while the RCS interlock ensures that there is no prompt radiation through temporary penetrations, including the transport shaft and unsealed conduits. Before the transition to an installation shift, a radiation survey is done and areas of radio-activation are secured. During the installation shift, daily work control planning is implemented for all tasks in the linac tunnel, with specified locations, times, and personnel. When switching back to commissioning, the operator-in-charge ensures that the operational conditions are restored and search-and-evict is conducted following the established procedures.

MAINTENANCE INFRASTRUCTURE

To facilitate future maintenance and development, a new 1440 m² cryogenic assembly building (CAB) is being constructed (Fig. 1) to provide additional space for development and production of cryogenic systems, cryomodules, and superconducting magnets. The CAB is adjacent to the 2500 m² “SRF Highbay” [36] which supports the production throughput of testing five resonators per week and one cryomodule per month. In addition, an electro-polishing (EP) facility is being established to support the FRIB upgrade.

SUMMARY

Nearly five years after the start of technical construction, FRIB is progressing on schedule and on cost, with beam commissioning completed through the first 15 of 46 superconducting cryomodules, and with heavy ions of Ne, Ar, Kr and Xe accelerated above 20 MeV/u. The next phase of beam commissioning (ARR4) scheduled after March 2020 aims at accelerating these heavy ion beams to about 200 MeV/u using the 15 QWR CMs and 24 HWR CMs. Operations for scientific users is expected to start as planned in 2022.

ACKNOWLEDGMENTS

FRIB accelerator systems design and construction have been facilitated under work-for-others agreements with many DOE-SC national laboratories including ANL, BNL, FNAL, JLab, LANL, LBNL, ORNL, and SLAC, and in collaboration with institutes worldwide including BINP, KEK, IHEP, IMP, INFN, INR, RIKEN, TRIUMF, and Tsinghua University. The cryogenics system was developed in collaboration with the JLab cryogenics team. The SRF development benefited greatly from the expertise of the low- β SRF community. FRIB has been collaborating with ANL on RF coupler and tuner developments, assisted by JLAB for cryomodule design, and by FNAL and JLab on cavity treatments.

We thank the FRIB Accelerator Systems Advisory Committee for their valuable guidance, colleagues who participated in FRIB accelerator peer reviews including G. Ambrosio, J. Anderson, D. Arenius, W. Barletta, G. Bauer, G. Biallas, J. Bisognano, S. Bousson, P. Brindza, S. Caspi, M. Champion, D. Cossairt, M. Crofford, C. Cullen, D. Curry, R. Cutler, G. Decker, J. Delayen, J. Delong, G. Dodson, J. Donald, H. Edwards, J. Error, J. Fuerst, T. Khabiboulline, F. Kornegay, K. Kurukawa, J. Galambos, J. Galayda, G. Gassner, P. Ghoshal, J. Gilpatrick, C. Ginsburg, S. Gourlay, M. Harrison, S. Hartman, S. Henderson, G. Hoffstaetter, J. Hogan, S. Holmes, M. Howell, P. Hurh, R. Kersevan, A. Hodgkinson, N. Holtkamp, H. Horiike, C. Hovater, H. Imao, R. Janssens, R. Keller, J. Kelley, P. Kelley, J. Kerby, S.H. Kim, A. Klebaner, J. Knobloch, R. Lambiase, M. Lamm, Y. Li, C. LoCocq, C. Luongo, K. Mahoney, J. Mammosser, T. Mann, W. Meng, N. Mokhov, G. Murdoch, J. Nolen, W. Norum, H. Okuno, S. Ozaki, R. Pardo, S. Peggs, R. Petkus, C. Pearson, F. Pellemoine, T. Peterson, C. Piller, J. Power, T. Powers, J. Preble, J. Price, D. Raparia, J. Rathke, A. Ratti, T. Roser, M. Ross, R. Ruland, J. Sandberg, R. Schmidt, W.J. Schneider, D. Schrage, S. Sharma, I. Silverman, K. Smith, J. Sondericker, W. Soyars, C. Spencer, R. Stanek, M. Stettler, W.C. Stone, J. Stovall, H. Strong, L.T. Sun, Y. Than, J. Theilacker, Y. Tian, M. Thuot, J. Tuozzolo, V. Verzilov, R. Vondrasek, P. Wanderer, K. White, P. Wright, H. Xu, L. Young, and A. Zaltsman, and colleagues who advised and collaborated with the FRIB team including A. Burrill, A.C. Crawford, K. Davis, X. Guan, P. He, Y. He, A. Hutton, P. Kneisel, R. Ma, K. Macha, G. Maler, E.A. McEwen, S. Prestemon, J. Qiang, T. Reilly, R. Talman, J. Vincent, X.W. Wang, J. Xia, Q.Z. Xing, and H.H. Zhang. The FRIB accelerator design is executed by a dedicated team in the FRIB Accelerator Systems Division with close collaboration with the Experimental Systems Division headed by G. Bollen, the Conventional Facility Division headed by B. Bull, and the Chief Engineer's team headed by D. Stout, with support from the FRIB project controls, procurement, and ES&H teams, and from NSCL and MSU.

REFERENCES

- [1] J. Wei *et al.*, "Advances of the FRIB project", *International Journal of Modern Physics E*, vol. 28, pp. 1930003-1-18, 2019.
- [2] J. Wei *et al.*, "The FRIB project – accelerator challenges and progress", in *Proc. HIAT'12*, Chicago, IL, USA, Jun. 2012, paper MOB01, pp. 8-19.
- [3] M. J. Johnson *et al.*, "Design of the FRIB cryomodule", in *Proc. IPAC'12*, New Orleans, LA, USA, May 2012, paper WEPPD006, pp. 2507-2509.
- [4] S. J. Miller *et al.*, "FRIB cavity and cryomodule performance, comparison with the design and lessons learned", presented at the SRF'19, Dresden, Germany, Jun.-Jul. 2019, paper WETEA5, this conference.
- [5] T. Xu *et al.*, "Progress of FRIB SRF production", in *Proc. SRF'17*, Lanzhou, China, Jul. 2017, pp. 345-352. doi:10.18429/JACoW-SRF2017-TUXAA03.
- [6] V. Ganni, P. Knudsen, D. Arenius, and F. Casagrande, "Application of JLab 12 GeV helium refrigeration system for the FRIB accelerator at MSU", in *Advances in Cryogenic Engineering*, vol. 59A, AIP Conference Proceedings 1573, edited by J.G. Weisend II *et al.* American Institute of Physics, Melville, NY, 2014, pp. 323–328.
- [7] A. Facco *et al.*, "Superconducting resonators development for the FRIB and ReA Linacs at MSU: recent achievements and future goals", in *Proc. IPAC'12*, New Orleans, LA, USA, May 2012, paper MOOAC03, pp. 61-63.
- [8] A. Facco *et al.*, "Faced issues in ReA3 quarter-wave resonators and their successful resolution", in *Proc. SRF'13*, Paris, France, Sep. 2013, paper THIOD02, pp. 873-877.
- [9] S. Stark *et al.*, "FRIB HWR tuner development", in *Proc. LINAC'16*, East Lansing, MI, USA, Sep. 2016, pp. 535- 537. doi:10.18429/JACoW-LINAC2016-TUPLR029.
- [10] S. J. Miller *et al.*, "Low-beta cryomodule design optimized for large-scale linac installations", in *Proc. SRF'13*, Paris, France, Sep. 2013, paper THIOA04, pp. 825-829.
- [11] M. Ikegami, "Machine and personnel protection for high power hadron linacs", in *Proc. IPAC'15*, Richmond, VA, USA, May 2015, pp. 2418-2422. doi:10.18429/JACoW-IPAC2015-WEXC1.
- [12] F. Casagrande, "Cryogenics and cryomodule for large scale accelerators", presented at IPAC'15, Richmond, VA, USA, May 2015, talk THYB1, unpublished.
- [13] C. Compton *et al.*, "The FRIB superconducting cavity production status and findings concerning surface defects", presented at the SRF'19, Dresden, Germany, Jun.-Jul. 2019, paper THP098, this conference.
- [14] E. S. Metzgar and L. Popielarski, "Summary of FRIB cavity processing in the SRF coldmass processing facility and lessons learned", presented at the SRF'19, Dresden, Germany, Jun.-Jul. 2019, paper TUP093, this conference.
- [15] W. Hartung *et al.*, "Performance of FRIB production quarter-wave and half-wave resonators in dewar certification tests", presented at the SRF'19, Dresden, Germany, Jun.-Jul. 2019, paper THP061, this conference.
- [16] K. Elliott and L. Popielarski, "Experiences of superconducting radio frequency coldmass production for the FRIB linear accelerator", presented at the SRF'19, Dresden, Germany, Jun.-Jul. 2019, paper TUP092, this conference.
- [17] W. Chang *et al.*, "Progress in FRIB cryomodule bunker tests", presented at the SRF'19, Dresden, Germany, Jun.- Jul. 2019, paper THP062, this conference.

- Content from this work may be used under the terms of the CC BY 3.0 licence (© 2019). Any distribution of this work must maintain attribution to the author(s), title of the work, publisher, and DOI.
- [18] J. T. Popielarski *et al.*, “FRIB coupler performance and lessons learned”, presented at the SRF'19, Dresden, Germany, Jun.-Jul. 2019, paper MOP071, this conference.
- [19] K. Saito *et al.*, “FRIB solenoid package in cryomodule and local magnetic shield”, presented at the SRF'19, Dresden, Germany, Jun.-Jul. 2019, paper MOP072, this conference.
- [20] M. Xu *et al.*, “FRIB LS1 cryomodule's solenoid commissioning”, presented at the SRF'19, Dresden, Germany, Jun.-Jul. 2019, paper TUP089, this conference.
- [21] C. Compton *et al.*, “Production status of superconducting cryomodules for the Facility for Rare Isotope Beams”, presented at the SRF'19, Dresden, Germany, Jun.-Jul. 2019, paper TUP091, this conference.
- [22] S. H. Kim *et al.*, “Performance of Quarter Wave Resonators in the FRIB Superconducting Driver Linear Accelerator”, presented at the SRF'19, Dresden, Germany, Jun.-Jul. 2019, paper TUP090, this conference.
- [23] D. G. Morris *et al.*, “RF System for FRIB accelerator”, in *Proc. IPAC'18*, Vancouver, Canada, Apr.-May 2018, pp. 1765-1770. doi:10.18429/JACoW-IPAC2018-WEXGBF3.
- [24] J. Vincent *et al.*, “On active disturbance rejection based control design for superconducting RF cavities”, *Nucl. Instrum. Meth. Phys. Res. A*, vol. 643, pp. 11-16, 2011.
- [25] J. L. Crisp *et al.*, “Beam position and phase measurements of microampere beams at the Michigan State University ReA3 facility”, in *Proc. NAPAC'13*, Pasadena, CA, USA, Sep.-Oct. 2013, paper THPAC20, pp. 1187-1189.
- [26] Z. Liu, J. L. Crisp, T. Russo, R. C. Webber, and Y. Zhang, “A new beam loss detector for low-energy proton and heavy-ion accelerators”, *Nucl. Instrum. Meth. Phys. Res. A*, vol. 767, pp. 262, 2014.
- [27] *7th MicroTCA Workshop for Industry and Research*, Hamburg, Germany, 2018, <https://mtcaws.desy.de>
- [28] S. Cogan, S. M. Lidia, and R. C. Webber, “Diagnostic data acquisition strategies at FRIB”, in *Proc. IBIC'16*, Barcelona, Spain, Sep. 2016, pp. 572-576. doi:10.18429/JACoW-IBIC2016-WEAL03.
- [29] M. G. Konrad, “Timing and synchronization at FRIB”, in *Proc. PCaPAC'16*, Campinas, Brazil, Oct. 2016, pp. 105-107. doi:10.18429/JACoW-PCaPAC2016-THPOPRP010
- [30] Z. Li, D. Chabot, S. Cogan, S. M. Lidia, and R. C. Webber, “FRIB fast machine protection system: chopper monitor system design”, in *Proc. LINAC'18*, Beijing, China, Sep. 2018, pp. 336-338. doi:10.18429/JACoW-LINAC2018-TUP0007.
- [31] S. M. Lidia, “Diagnostics for high power accelerator machine protection systems”, in *Proc. IBIC'14*, Monterey, CA, USA, Sep. 2014, paper TUIYB1, pp. 239-249.
- [32] Z. Li, L. R. Dalesio, M. Ikegami, S. M. Lidia, L. Wang, and S. Zhao, “FRIB fast machine protection system: engineering for distributed fault monitoring system and light speed response”, in *Proc. LINAC'16*, East Lansing, MI, USA, Sep. 2016, pp. 959-961. doi:10.18429/JACoW-LINAC2016-THPLR046.
- [33] M. G. Konrad, D. G. Maxwell, and G. Shen, “Continuous integration and continuous delivery at FRIB”, in *Proc. PCaPAC'16*, Campinas, Brazil, Oct. 2016, pp. 145-147. doi:10.18429/JACoW-PCaPAC2016-FRITPLC001.
- [34] E. Pozdeyev *et al.*, “First acceleration at FRIB”, in *Proc. LINAC'18*, Beijing, China, Sep. 2018, pp. 615-619. doi:10.18429/JACoW-LINAC2018-WE2A01.
- [35] P. Ostroumov *et al.*, “Heavy ion beam acceleration in the first three cryomodules at the Facility for Rare Isotope Beams at Michigan State University”, *Phys. Rev. Accel. Beams*, vol. 22, 040101-1-12, 2019.
- [36] L. Popielarski *et al.*, “SRF Highbay technical infrastructure for FRIB production at Michigan State University”, in *Proc. LINAC'14*, Geneva, Switzerland, Aug.-Sep. 2014, paper THPP046, pp. 954-956.